HHS Public Access

Author manuscript

Biomaterials. Author manuscript; available in PMC 2016 September 01.

Published in final edited form as:

Biomaterials. 2015 September ; 63: 137–145. doi:10.1016/j.biomaterials.2015.06.025.

Simple Coating with Fibronectin Fragment Enhances Stainless Steel Screw Osseointegration in Healthy and Osteoporotic Rats

Rachit Agarwal[1], **Cristina González-García**[1,2], **Brennan Torstrick**[1], **Robert E. Guldberg**[1], **Manuel Salmerón-Sánchez**[2], and **Andrés J. García**[1,#]

[1]Woodruff School of Mechanical Engineering and Petit Institute for Bioengineering and Bioscience, Georgia Institute of Technology, Atlanta, GA, USA

[2]Biomedical Engineering Research Division, University of Glasgow, Glasgow, UK

Abstract

Metal implants are widely used to provide structural support and stability in current surgical treatments for bone fractures, spinal fusions, and joint arthroplasties as well as craniofacial and dental applications. Early implant-bone mechanical fixation is an important requirement for the successful performance of such implants. However, adequate osseointegration has been difficult to achieve especially in challenging disease states like osteoporosis due to reduced bone mass and strength. Here, we present a simple coating strategy based on passive adsorption of FN7-10, a recombinant fragment of human fibronectin encompassing the major cell adhesive, integrin-binding site, onto 316-grade stainless steel (SS). FN7-10 coating on SS surfaces promoted α5β1 integrin-dependent adhesion and osteogenic differentiation of human mesenchymal stem cells. FN7-10-coated SS screws increased bone-implant mechanical fixation compared to uncoated screws by 30% and 45% at 1 and 3 months, respectively, in healthy rats. Importantly, FN7-10 coating significantly enhanced bone-screw fixation by 57% and 32% at 1 and 3 months, respectively, and bone-implant ingrowth by 30% at 3 months compared to uncoated screws in osteoporotic rats. These coatings are easy to apply intra-operatively, even to implants with complex geometries and structures, facilitating the potential for rapid translation to clinical settings.

Keywords

integrin; cell adhesion; bone; implant

[#]Corresponding Author: Andrés J. García, Ph.D., F.B.S.E., Rae S. and Frank H. Neely Chair and Regents' Professor, Woodruff School of Mechanical Engineering, Petit Institute for Bioengineering and Bioscience, Georgia Institute of Technology, 2310 IBB Building, 315 Ferst Drive, Atlanta, GA 30332-0363, phone: 404-894-9384, andres.garcia@me.gatech.edu.

INTRODUCTION

Metal implants are widely used in current surgical treatments for bone fractures, spinal fusions, and joint arthroplasties as well as craniofacial and dental applications. In particular, stainless steel (SS) plates, screws and pins are extensively used as bone fracture fixation devices due their mechanical properties, corrosion resistance and cost effectiveness when compared to other metallic implants [1, 2]. For example, stainless steel has improved shear strength compared to titanium. SS fracture fixation devices are conventional treatments for fractures in osteoporotic patients, which accounted for >2 million fractures in the USA at a cost of an estimated $19B [1]. The major problem in the management of osteoporotic fractures, which are characterized by poor bone stock with decreased implant pull-out strength, is unstable fixation arising from screw loosening and cutout, with rates ranging from 5–23% [3–5]. Similarly, transpedicular screw fixation represents the gold standard in the treatment of spinal deformities, spondylolisthesis, traumatic fractures, and reconstructions after spinal tumor resection [6, 7]. Furthermore, metal instrumentation is increasingly used in spinal fusions to improve stability and enhance fusion rates [6, 8]. Pedicle screw loosening represents a major complication of these spinal fixation procedures. Studies with well-defined radiological criteria documented high (18–27%) loosening rates [9–11]. In addition to contributing to instrumentation breakage and failure (11% incidence [12]), screw loosening results in pain, loss of spinal alignment, and increased incidence of pseudoarthrosis [9, 13]. Screw loosening has a significant higher incidence in fixation of vertebral bodies with low mineral density or in patients with osteoporosis, neuromuscular disorders, or post-radiation therapy [14, 15].

Various strategies have been explored to enhance osseointegration of metal implants [16–21]. Surface roughness has been shown to increase osteoblast differentiation and mineralization [18, 22]. Additionally, increased surface roughness results in production of phospholipase A2 in osteoblasts which then catalyzes prostaglandin E2 and makes osteoblasts responsive to systemic hormones such as 1,25-$(OH)_2D_3$ [16]. Hydrofluoric acid-etched titanium implants exhibited significantly higher bone-implant contact compared to non-treated implants in rat tibiae [23]. Similarly, acid etched screws implanted in rabbit distal femurs had enhanced osseointegration compared to machined screws [18]. In contrast, Kang *et al.* implanted SS mini screws that were either machined or laser-surface treated in the maxilla of dogs and found no improvements in bone-implant contact [24]. Similarly, rough and smooth SS pegs implanted in the distal femur of rabbits showed no differences in osseointegration [25]. These studies highlight the difficulties in identifying surface roughness/topography parameters needed for enhanced osseointegration [26]. Reproducible surface roughness is difficult to produce due to use of different instruments and techniques, as well as complex geometries associated with dental and orthopaedic devices, and hence there is wide inconsistency across published studies [26, 27]. Hydroxyapatite (HA) and other calcium phosphate (CaP) coatings applied to implant surfaces have also been shown to promote osseointegration [28–31]. HA-coated implants bridge 1–2 mm gaps between implant and bone and had higher bone in-growth compared to uncoated implants when implanted in femoral condyles of dogs [19]. Titanium implants with CaP coatings showed significantly higher bone contact in goat femoral diaphysis compared to uncoated implants

at 6-, 12- and 24-weeks [32]. However, such coatings are often mechanically unstable and difficult to apply uniformly on implants with complex shapes, thereby limiting their use [33, 34]. Bisphosphonates have been proposed to enhance osseointegration of implants in healthy and osteoporotic bone [35–40]. Bisphosphonates reduce early stage resorption of bone caused by surgical and implantation trauma by inhibiting osteoclasts [36]. Bisphosphonate coatings on dental titanium implants in human maxilla result in improved fixation [41]. These coating procedures, however, are fairly complex and require chemical modification of implants [35, 37, 41]. Furthermore, systemic use of bisphosphonates has been linked to higher risk of atypical femoral fractures in women [42] raising safety concerns.

Despite this progress, there is still a significant and unmet need to improve the integration of metal implants and bone, especially in clinically challenging scenarios such as osteoporosis due to low bone mass density and strength [43, 44]. To enhance implant-bone integration, presentation of adhesion motifs from extracellular matrix proteins that bind integrin adhesion receptors on implant surfaces has been proposed [45–53]. We previously showed that presentation of a recombinant fragment spanning the 7–10th type III repeats of human fibronectin (FN7-10), which contains the integrin-binding RGD site in the 10th type III repeat and PHSRN synergy site in the 9th type III repeat, on titanium implants improved bone-implant contact and mechanical fixation in healthy rats [51, 53]. However, the efficacy of integrin-specific coatings on improving osseointegration in disease models such as osteoporosis has not been tested. The objectives of this study were to apply FN7-10 coatings by a simple one-step passive adsorption onto clinical grade SS implant and evaluate the effects of these coatings on implant osseointegration in healthy and osteoporotic rats.

METHODS

Recombinant FN7-10 production

FN7-10 was expressed in *E. coli* and purified as previously described [54]. Briefly, JM109 bacterial cells containing the FN7-10 construct were streaked onto lysogeny broth (LB) agar plates containing 100 mg/mL ampicillin and incubated overnight. Colonies were isolated and dynamically cultured in LB broth (100 mg/mL ampicillin; 2 mM d-biotin). At 6 h, 100 mM isopropylthio-β-galactoside (IPTG) was added to augment protein production. The culture was spun down at 4000*g* for 10 min at 4 °C, and the cell pellet was lysed using bacterial protein extraction reagent (B-Per™, Life Technologies, Carlsbad, CA, USA). The lysate was centrifuged (10,000*g*) for 20 min. The protein supernatant was sterile-filtered, and purified by affinity chromatography using a 5 mL column of Ultralink Immobilized Monomeric Avidin (Life Technologies) and eluted using d-biotin. After removing d-biotin using 30 kDa Microcon centrifugal filter devices (Millipore, Billerica, MA, USA), protein fractions were sterile-filtered. Purified protein was verified by Western blotting and enzyme-linked immunosorbent assay (ELISA), and endotoxin levels were below the recommended maximum FDA level (0.5 EU/ml) as determined by the Limulus Amebocyte Lysate (LAL) chromogenic assay.

SS samples and coating

SS plates (25 mm × 25 mm × 0.5 mm) were purchased from Goodfellow (Coraopolis, PA, USA). Surfaces were cleaned in Piranha solution for 30 min and sterilized by autoclaving. FN7-10 coatings were generated by incubating SS samples in purified solutions of FN7-10 in PBS for 30 min at room temperature. The density of adsorbed FN7-10 was quantified by ELISA [55]. Briefly, SS samples were incubated in varying concentrations of FN7-10 and washed multiple times with 0.05% v/v Triton-X-100 in PBS. Samples were then incubated in 1% w/v casein blocker (Life Technologies) and probed with 1 μg/mL HFN7.1 antibody (Developmental Hybridoma Studies Bank, Iowa City, Iowa, USA). HFN 7.1 binds between the 9^{th} and 10^{th} type III repeat of fibronectin and blocks cell adhesion to the central integrin-binding site [55]. After several washes, samples were incubated in alkaline phosphatase (ALP)-conjugated antibody (1 μg/mL). Following several washes, samples were incubated with 5-methyl umbelliferyl phosphate substrate (60 μg/mL) and fluorescence read at excitation/emission of 360 nm/465 nm on a HTS 7000 Plus plate reader (Perkin Elmer, Akron, Ohio, USA). Absolute values of adsorbed FN7-10 were determined by comparing fluorescence readings to reference titanium samples coated with FN7-10 [53]. For cell experiments, SS samples were coated with 50 μg/mL FN7-10 for 30 min to generate a saturated FN7-10 monolayer.

Cell adhesion and osteoblastic differentiation

Human mesenchymal stem cells (hMSCs) were obtained from the Institute of Regenerative Medicine at Texas A&M (College Station, TX, USA) cultured in Lonza mesenchymal stem cell medium (MSCM) and SingleQuots, and passaged every 3 to 4 days. hMSCs were seeded on SS samples that were either coated with FN7-10 or incubated in PBS (uncoated) in a 12-well plate. Each SS sample was seeded with 10,000 cells. Cells were allowed to adhere in 10% v/v serum-containing media for 2 h at 37°C and 5% v/v CO_2. Samples were then washed with PBS, incubated in Calcein-AM (1 μg/mL, Life Technologies) to label live cells, and imaged using an upright fluorescent microscope. Five random images were taken per sample and analyzed for total cells and cell spread area using ImageJ software. For integrin blocking experiments, cells were labeled with Calcein-AM (1 μg/mL) for 15 min, incubated in the presence of 10 μg/mL anti-integrin α_5 (BIIG2, Developmental Studies Hybridoma Bank), 10 μg/mL anti-integrin $\alpha_v\beta_3$ (clone LM609, Millipore) or corresponding isotype control antibodies for 10 min prior to cell seeding, and seeded for 1 h in serum-containing media with 50,000 cells per sample. This time point was chosen to minimize antibody internalization. SS samples were then washed 3 times with PBS to remove poorly adherent cells and imaged using an upright fluorescence microscope.

For osteoblastic differentiation assays, hMSCs were plated at 10,000 cells/cm^2 onto FN7-10-coated and control uncoated SS samples in osteogenic differentiation media from Lonza (Allendale, NJ, USA). Alkaline phosphatase (ALP) activity was quantified at 9 days in culture [50]. Briefly, a probe sonicator was used to lyse cells, and equal protein amounts were added to 5-methyl umbelliferyl phosphate substrate (60 μg/mL) for 60 min. Fluorescence was measured (360 nm/465 nm) and enzymatic activity normalized to total amount of protein. Alizarin red staining was used to quantify mineralization [56]. hMSCs were cultured for 21 days on SS samples in osteogenic media. Cells were then fixed with

3.7% w/v formaldehyde for 20 min and stained with 40 mM Alizarin red (pH 4.1) for 20 min at room temperature. Samples were washed with water and incubated with 10% v/v acetic acid for 30 min. Stained surfaces were then scraped and transferred in a tube and heated at 85°C for 10 min. Resulting slurry was centrifuged at 18,000*g* for 10 minutes and supernatant was neutralized with 10% w/v ammonium hydroxide. Absorbance readings were taken at 405 nm.

Screw implantation

All experiments were conducted in accordance with an Institutional Animal Care and Use Committee (IACUC)-approved protocol. Female, 8–10 weeks old Sprague-Dawley rats were purchased from Harlan (Dublin, VA, USA) and used in two studies. For Study 1, healthy rats were used at the age of 10–12 weeks at the time of surgery. For Study 2, ovariectomized (OVX) or sham-operated animals (surgically operated similar to OVX rats except that the ovaries were not cauterized) were used three months after ovariectomy (age of 25–27 weeks at the time of surgery). Because ovariectomized rats have increased appetites and gain weight, animals were pair-fed daily to eliminate weight gain as a confounding variable [57]. The amount of food given to ovariectomized animals was similar to that consumed by sham-operated controls. The osteoporotic state in ovariectomized subjects was confirmed by micro-computed tomography (μCT) imaging of the proximal tibia [58]. For μCT scanning, a 3.125 mm length of that proximal tibia was scanned in anesthetized, live rats on the right leg using a VivaCT system (Scanco Medical, Wayne, PA, USA; 145 mA intensity, 55 kVp energy, 376 ms integration time, and 12.5 μm resolution). Bone structure was evaluated by contouring 2D slices to include only the trabecular bone. 3D μCT reconstructions were rendered and the ratio of bone volume to total volume was computed as a measure of osteoporotic state in ovariectomized rats with sham-operated animals as controls.

SS 316 grade M2 screws (McMaster Carr, Atlanta, GA, USA) (2.0 mm in thread length, 2 mm thread diameter) were cleaned with Piranha solution for 30 min and sterilized by autoclaving. Screws were then incubated in 50 μg/mL FN7-10 or PBS for 30 min at the time of surgery. For implantation, the proximal tibia was exposed by a 1.5 cm longitudinal incision through the skin. Muscle was separated using blunt dissection. Using a 1.7 mm diameter drill bit, a hole was made approximately 2–5 mm distal from the tibial metaphysis. Implants were screwed into the hole, muscle sutured and the skin closed via wound clips. Each rat received one screw per tibia (two per rat) with each animal receiving uncoated and FN7-10-coated screws with implant coating group randomized between left and right leg. A dose of sustained-release buprenorphine was administered immediately after anesthesia induction. The rats were allowed to bear weight immediately after surgery without any restrictions.

Osseointegration analysis

Animals were euthanized at either 4 or 12 weeks post-implantation, and tibiae harvested. Samples were either fixed in neutral-buffered formalin for histology or wrapped in PBS-soaked gauze to maintain moisture for immediate mechanical testing. For sectioning, explanted tibiae were fixed in neutral-buffered formalin and processed through ascending grades of ethanol followed by xylene before embedding in methyl methacrylate. After

embedding, rough sections were cut (Isomet® 1000 Precision Saw, Buehler, Lake Bluff, IL, USA) and ground to 50 μm (EXAKT 400 CS). Sections were stained using Sanderson's Rapid Bone Stain with a Van Gieson's counterstain to distinguish mineralized tissue (red) from other soft tissues. Images were taken using a Nikon Eclipse E600 and the fraction of area staining for bone within the screw thread was measured using ImageJ (NIH, Bethesda, MD, USA).

Pull-out testing was performed to quantify implant mechanical fixation to surrounding bone tissue using a MTS 858 Mini Bionix II (MTS Systems, Eden Prairie, MN, USA). The explanted tibia was secured using a customized holding apparatus, and the exposed head of the implant attached to a load cell via piano wire using a customized grip apparatus. Pre-loaded samples (1.0 N) were then subjected to a constant loading rate of 0.2 N/sec. The pull-out force (N), parallel to the long axis of implant, was the maximum load achieved before implant detachment or failure.

Statistics

Results are presented as mean and standard deviation. Results were analyzed by one-tailed Student's t-test in GraphPad and a confidence level of 95% was considered significant. All assays (except mechanical testing) were conducted at least in triplicate.

RESULTS

Passive adsorption of FN7-10 onto SS

Recombinant FN7-10 protein was produced with high purity (>95%) and biological activity as determined by gel staining, Western blotting, and ELISA using the HFN7.1 receptor-mimetic antibody, in excellent agreement with previous reports [51, 53, 54]. We examined the adsorption of FN7-10 onto SS from a pure FN7-10 solution using a modified ELISA. Passive adsorption of FN7-10 onto SS surfaces is expected to be driven by entropic displacement of water (hydrophobic interactions) and other non-covalent interactions (hydrogen bonding, electrostatic, etc). The adsorption profile for FN7-10 onto SS exhibited a hyperbolic dependence on FN7-10 coating concentration, with linear increases at low FN7-10 concentrations and reaching saturated levels at around 30 μg/mL (Fig. 1). A coating concentration of 50 μg/mL was selected for all subsequent experiments which resulted in a surface density of 56.1 ± 5.3 ng/cm^2 (1.1 ± 0.10 pmol/cm^2). The adsorption profile for SS shown in Figure 1 is consistent with that of titanium previously reported [53]. At a coating concentration of 50 μg/mL, FN7-10 surface density is similar for both surfaces: 1.1 ± 0.1 pmol/cm^2 for SS vs 1.4 ± 0.2 pmol/cm^2 for titanium.

FN7-10 coating promotes hMSC cell adhesion and osteoblastic differentiation

hMSCs were cultured on FN7-10-coated and uncoated SS surfaces in serum-containing media. hMSCs express high levels of several fibronectin-binding integrins including $\alpha_5\beta_1$ [59]. Cells cultured on FN7-10-coated SS surfaces had higher adhesion levels at 1 h compared to uncoated surfaces (Fig. 2). Cell adhesion density was two-fold higher on FN7-10-coated SS compared to uncoated SS (Fig. 2C) ($p<0.002$). Cells on FN7-10-coated SS also had higher spread area than cells on uncoated SS (Fig. 2D) ($p<0.03$). Blocking

studies with integrin-specific antibodies demonstrated that hMSCs primarily adhere to FN7-10-coated SS via the $\alpha_5\beta_1$ integrin ($p<0.0001$) (Fig. 3A). In contrast, hMSC adhesion to uncoated SS was not blocked by $\alpha_5\beta_1$-blocking antibodies (Fig. 3B). Cell adhesion to uncoated SS most likely involves integrin binding to adsorbed serum proteins such as vitronectin that bind α_V integrins. An $\alpha_V\beta_3$-blocking antibody partially reduced hMSC adhesion to uncoated SS compared to the isotype control ($p<0.05$). These results demonstrate that hMSC interact with FN7-10-coated SS primarily via $\alpha_5\beta_1$ integrin, whereas cells adhere to uncoated SS using different integrins, including $\alpha_V\beta_3$.

Binding of $\alpha_5\beta_1$ to fibronectin in hMSCs promotes differentiation towards the osteogenic lineage [59, 60]. To evaluate the effect of FN7-10-coated SS on osteoblastic differentiation, we cultured hMSCs on SS in osteogenic media for 9 days after which the cells were lysed and quantified for ALP activity, an early marker for osteogenic differentiation [61]. Cells cultured on FN7-10-coated SS had 3-fold higher levels of ALP activity compared to cells on uncoated surfaces (Fig. 4A) ($p<0.006$). We also examined matrix mineralization via Alizarin red staining as a mature marker of osteoblastic differerentiation [56]. Consistent with ALP activity results, hMSCs cultured on FN7-10-coated surfaces exhibited significantly higher mineralization than cells cultured on uncoated SS at 21 days (Fig. 4B) ($p<0.02$).

FN7-10 coating enhances SS implant osseointegration in healthy rats

We previously showed that FN7-10 coatings enhance bone-implant contact and mechanical fixation of commercially pure, machine-finished titanium rods in healthy rats [53]. In the current study, we first evaluated the effect of FN7-10 coating on the osseointegration of SS screws implanted in the tibiae of healthy rats. SS screws were coated with FN7-10 by simply incubating in FN7-10 solution for 30 min prior to surgery, and one screw was implanted in the tibial metaphysis of each leg. At 1 and 3 months after the implantation, rats were euthanized and implant-bone pull-out force was measured. FN7-10-coated SS screws exhibited 30% higher pull-out force than uncoated screws at 1 month of implantation ($p<0.01$) (Fig. 5A). Similarly, FN7-10 coating enhanced the mechanical fixation of SS screws to bone at 3 months by 45% compared to uncoated screws ($p<0.03$) (Fig. 5B).

FN7-10 coating enhances osseointegration of SS screws in osteoporotic rats

Osteoporosis leads to destruction of bone microstructure and trabecular bone [62], and these reductions in bone mass lead to increased risk for fractures. Importantly, loss of bone mass results in weak osseointegration of implants [43, 44]. To test whether FN7-10 coating on SS enhances implant osseointegration in this challenging diseased state, we used ovariectomized rats as a model of osteoporosis [63]. To confirm osteoporosis, live animal μCT was performed 3 months after ovariectomy. The ratio of bone volume to total volume (BV/TV) in the tibial metaphysis was calculated for ovariectomized and sham-operated control rats. μCT analyses demonstrated significant reductions in the trabecular bone volume fraction of ovariectomized rats (BV/TV: 0.09±0.03) compared to sham-operated rats (BV/TV: 0.33±0.07) ($p < 0.001$) (Fig. 6).

Following confirmation of osteoporosis, we implanted FN7-10-coated and uncoated SS screws in both osteoporotic and sham-operated rats. For both osteoporotic and sham-

operated rats, FN7-10-coated SS screws exhibited significantly higher mechanical fixation at 1 and 3 months post-implantation compared to uncoated screws (Fig. 7). Importantly, FN7-10 coatings enhanced SS screw-bone pull-out force by 57% ($p<0.03$) and 32% ($p<0.05$) over uncoated screws in osteoporotic rats at 1 and 3 months, respectively (Fig. 7A). The observed increases in pull-out force for FN7-10-coated screws compared to uncoated screws for sham-operated controls (Fig. 7B) are consistent with the enhancements in mechanical fixation in naïve, healthy rats (Fig. 5). Taken together, these results demonstrate that FN7-10 coatings applied to SS screws significantly enhance bone-implant mechanical fixation in both healthy and osteoporotic rats.

Histological sections were also generated and stained to evaluate bone-metal contact and bone ingrowth into thread regions at the interface of screw and bone for osteoporotic rats. Overall, SS screws were well tolerated and remained in close apposition to the cortical bone for all groups. No evidence of foreign body giant cells or fibrous capsule was observed in any of the histological sections. We performed histomorphometric analyses to quantify bone ingrowth into the screw threads. Consistent with the enhancements in screw mechanical fixation, a 30% increase in bone ingrowth was observed for FN7-10-coated screws compared to uncoated screws ($p<0.003$) (Fig. 8).

DISCUSSION

In the present study, we show that simple adsorption of the recombinant fibronectin fragment FN7-10 onto SS significantly enhances hMSC adhesion and osteoblastic differentiation. Importantly, this simple coating process also enhances the mechanical fixation and bone-implant contact of SS screws in healthy and osteoporotic rats. Blocking studies with integrin-specific antibodies demonstrated that hMSCs primarily adhere to FN7-10-coated SS via the $\alpha_5\beta_1$ integrin, whereas cells adhere to uncoated SS using different integrins, including $\alpha_V\beta_3$. We previously showed that integrin binding specificity and signaling via $\alpha_5\beta_1$ integrin regulates osteoblastic differentiation and osseointegration of smooth titanium implants [51, 64]. An important aspect of the present study is that these integrin-specific coatings were generated by simple passive adsorption (30 min) from solution. This facile coating strategy can be easily applied to metal implants and devices with complex geometries and structures. Additionally, the coating can be simply applied to any device at the time of surgery in a point-of-care application. Such simple application contrasts with other coating strategies focused on calcium-phosphate ceramics and polymers for drug delivery which require direct modification of the device prior to surgery, challenges with manufacturing, processing and sterilization, particularly for complex geometrical shapes and structures, and potential batch-to-batch variability [30]. For instance, calcium-phosphate coatings are applied using techniques such as pulsed laser deposition, sputter deposition, and ion beam deposition which lead to non-uniform deposition on screws [33]. Although the initial FN7-10 surface density can be easily controlled (Fig. 1), it is unlikely that FN7-10 will remain on the implant surface long-term. However, we expect that cells at the implant interface remodel the coating and deposit matrix that promotes bone formation and integration. As such, we hypothesize that this cell adhesive coating initiates pro-healing responses at the surface of the implant that result in enhanced implant-bone integration.

The major contribution of this study is the successful application of this simple coating strategy to improve implant osseointegration in a model of osteoporosis. This is a highly significant finding as the previous work using passive adsorption of ECM proteins has been done only with healthy subjects and demonstrating that this simple strategy is effective in a diseased state has considerable impact. Notably, the present study is the first report showing that an adhesive peptide-based strategy enhances SS implant osseointegration in an osteoporotic model. CaP and bisphosphonate coatings have shown improved osseointegration in osteoporotic bone [65], however simple passive adsorption of FN7-10 has significant advantages over complex coating strategies utilized for calcium phosphate-based and bisphosphonate coatings.

The main objective of the present study was to examine whether this simple, integrin-specific coating enhances bone-implant integration in conditions where the bone is compromised such as osteoporosis. The most significant problem in the management of osteoporotic fractures, which are characterized by poor bone stock with decreased implant pull-out strength, is unstable fixation arising from screw loosening [3–5]. Similarly, pedicle screw loosening represents a major complication of spinal fixation procedures, particularly in osteoporotic patients [66, 67]. We show that simple adsorption of FN7-10 on 316-grade SS leads to significant enhancements in mechanical fixation to bone at early (1 month) and late time points (3 month). Furthermore, FN7-10 coatings increased bone ingrowth into the screw threads compared to untreated screws. Future studies on large animals are necessary to establish the potential of this simple coating strategy for use in clinical settings.

We note that the pull-out force for uncoated and FN7-10-coated screws for sham-operated rats was less than healthy rats at 1 month implantation. However, by the end of 3 month time point, the pull-out forces were equivalent. We attribute the differences at the early time point to age differences at the time of screw implantation as sham-operated rats were 6–7 months old while healthy rats were 3 months old. It has been previously shown that aged rodents have reduced healing response to bone fractures compared to young healthy rodents [68]. Additionally, for osteoporotic rats, pull-out forces were consistently lower compared to sham-operated and healthy rats at both 1 and 3 month time points. Although FN7-10 coatings led to significant enhancement in pull-out forces in osteoporotic rats, the resulting forces were 25% lower than those for sham-operated rats. This difference in pull-out forces reflects the poor mechanical properties and limited osseointegrative potential of osteoporotic bone.

CONCLUSION

We demonstrate that simple adsorption of the recombinant fibronectin fragment FN7-10 onto SS promotes $\alpha_5\beta_1$ integrin-dependent adhesion and osteogenic differentiation of hMSCs. Importantly, FN7-10-coated SS screws significantly enhanced bone-implant mechanical fixation and bone contact in both healthy and osteoporotic rats. These coatings are easy to apply intra-operatively, even to implants with complex geometries and structures, facilitating the potential for rapid translation to clinical settings.

Acknowledgments

This work is supported by NIH grant R01 AR062920 and the Marie Curie Fellowship Program (IOF-Marie Curie Protdel 331655). We thank Angela Lin for help with μCT and pull-out measurements and GTRI and ME machine shops for their assistance in processing of SS implants. The HFN7.1 monoclonal antibody developed by RJ Klebe was obtained from the Developmental Studies Hybridoma Bank, created by the NICHD of the NIH and maintained at The University of Iowa, Department of Biology, Iowa City, IA 52242. hMSCs were provided by the Texas A&M Health Science Center College of Medicine Institute for Regenerative Medicine at Scott & White through a grant from ORIP of the NIH grant P40OD011050.

References

1. Muller R, Abke J, Schnell E, Macionczyk F, Gbureck U, Mehrl R, et al. Surface engineering of stainless steel materials by covalent collagen immobilization to improve implant biocompatibility. Biomaterials. 2005; 26:6962–72. [PubMed: 15967497]
2. Disegi JA, Eschbach L. Stainless steel in bone surgery. Injury. 2000; 31 (Suppl 4):2–6. [PubMed: 11270076]
3. Stromsoe K. Fracture fixation problems in osteoporosis. Injury. 2004; 35:107–13. [PubMed: 14736465]
4. Lindner T, Kanakaris NK, Marx B, Cockbain A, Kontakis G, Giannoudis PV. Fractures of the hip and osteoporosis: the role of bone substitutes. J Bone Joint Surg Br. 2009; 91:294–303. [PubMed: 19258602]
5. Moroni A, Hoang-Kim A, Lio V, Giannini S. Current Augmentation Fixation Techniques for the Osteoporotic Patient. Scandinavian Journal of Surgery. 2006; 95:103–9. [PubMed: 16821653]
6. Rutherford EE, Tarplett LJ, Davies EM, Harley JM, King LJ. Lumbar spine fusion and stabilization: hardware, techniques, and imaging appearances. Radiographics. 2007; 27:1737–49. [PubMed: 18025515]
7. Moshirfar A, Rand FF, Sponseller PD, Parazin SJ, Khanna AJ, Kebaish KM, et al. Pelvic fixation in spine surgery. Historical overview, indications, biomechanical relevance, and current techniques. J Bone Joint Surg Am. 2005; 87 (Suppl 2):89–106. [PubMed: 16326728]
8. Gibson JNA, Grant IC, Waddell G. The Cochrane Review of Surgery for Lumbar Disc Prolapse and Degenerative Lumbar Spondylosis. Spine. 1999; 24:1820. [PubMed: 10488513]
9. Pihlajamaki H, Myllynen P, Bostman O. Complications of transpedicular lumbosacral fixation for non-traumatic disorders. J Bone Joint Surg Br. 1997; 79:183–9. [PubMed: 9119839]
10. Soini J, Laine T, Pohjolainen T, Hurri H, Alaranta H. Spondylodesis augmented by transpedicular fixation in the treatment of olisthetic and degenerative conditions of the lumbar spine. Clin Orthop Relat Res. 1993; 297:111–6. [PubMed: 8242917]
11. Ohlin A, Karlsson M, Duppe H, Hasserius R, Redlund-Johnell I. Complications after transpedicular stabilization of the spine. A survivorship analysis of 163 cases. Spine. 1994; 19:2774–9. [PubMed: 7899978]
12. Renner SM, Lim TH, Kim WJ, Katolik L, An HS, Andersson GB. Augmentation of pedicle screw fixation strength using an injectable calcium phosphate cement as a function of injection timing and method. Spine. 2004; 29:E212–6. [PubMed: 15167670]
13. Sanden B, Olerud C, Petren-Mallmin M, Johansson C, Larsson S. The significance of radiolucent zones surrounding pedicle screws. Definition of screw loosening in spinal instrumentation. J Bone Joint Surg Br. 2004; 86:457–61. [PubMed: 15125138]
14. Halvorson TL, Kelley LA, Thomas KA, Whitecloud TS 3rd, Cook SD. Effects of bone mineral density on pedicle screw fixation. Spine. 1994; 19:2415–20. [PubMed: 7846594]
15. Weinstein JN, Spratt KF, Spengler D, Brick C, Reid S. Spinal pedicle fixation: reliability and validity of roentgenogram-based assessment and surgical factors on successful screw placement. Spine. 1988; 13:1012–8. [PubMed: 3206294]
16. Boyan BD, Sylvia VL, Liu Y, Sagun R, Cochran DLH, Lohmann C, et al. Surface roughness mediates its effects on osteoblasts via protein kinase A and phospholipase A2. Biomaterials. 1999; 20:2305–10. [PubMed: 10614936]

17. Klokkevold PR, Johnson P, Dadgostari S, Davies JE, Caputo A, Nishimura RD. Early endosseous integration enhanced by dual acid etching of titanium: a torque removal study in the rabbit. Clinical Oral Implants Research. 2001; 12:350–7. [PubMed: 11488864]
18. Wennerberg A, Albrektsson T. Suggested guidelines for the topographic evaluation of implant surfaces. The International journal of oral & maxillofacial implants. 2000; 15:331–44. [PubMed: 10874798]
19. Soballe K. Hydroxyapatite ceramic coating for bone implant fixation. Mechanical and histological studies in dogs. Acta orthopaedica Scandinavica Supplementum. 1993; 255:1–58. [PubMed: 8237337]
20. Cook SD, Thomas KA, Dalton JE, Volkman TK, Whitecloud TS 3rd, Kay JF. Hydroxylapatite coating of porous implants improves bone ingrowth and interface attachment strength. J Biomed Mater Res. 1992; 26:989–1001. [PubMed: 1429760]
21. Agarwal R, García AJ. Biomaterial strategies for engineering implants for enhanced osseointegration and bone repair. Advanced Drug Delivery Reviews. doi:101016/jaddr201503013.
22. Le Guehennec L, Soueidan A, Layrolle P, Amouriq Y. Surface treatments of titanium dental implants for rapid osseointegration. Dent Mater. 2007; 23:844–54. [PubMed: 16904738]
23. Cooper LF, Zhou Y, Takebe J, Guo J, Abron A, Holmen A, et al. Fluoride modification effects on osteoblast behavior and bone formation at TiO2 grit-blasted c.p. titanium endosseous implants. Biomaterials. 2006; 27:926–36. [PubMed: 16112191]
24. Kang HK, Chu TM, Dechow P, Stewart K, Kyung HM, Liu SS. Laser-treated stainless steel mini-screw implants: 3D surface roughness, bone-implant contact, and fracture resistance analysis. European journal of orthodontics. 2015
25. Imade S, Mori R, Uchio Y, Furuya S. Effect of implant surface roughness on bone fixation: the differences between bone and metal pegs. J Orthop Sci. 2009; 14:652–7. [PubMed: 19802680]
26. Shalabi MM, Gortemaker A, Hof MAVt, Jansen JA, Creugers NHJ. Implant Surface Roughness and Bone Healing: a Systematic Review. Journal of Dental Research. 2006; 85:496–500. [PubMed: 16723643]
27. Junker R, Dimakis A, Thoneick M, Jansen JA. Effects of implant surface coatings and composition on bone integration: a systematic review. Clin Oral Implants Res. 2009; 20 (Suppl 4):185–206. [PubMed: 19663965]
28. Valentin MI. Coatings based on calcium phosphates for metallic medical implants. Russian Chemical Reviews. 2013; 82:131.
29. Elyada A, Garti N, Furedi-Milhofer H. Polyelectrolyte multilayer - calcium phosphate composite coatings for metal implants. Biomacromolecules. 2014
30. de Groot K, Wolke JG, Jansen JA. Calcium phosphate coatings for medical implants. Proc Inst of Mech Eng H J Eng Med. 1998; 212:137–47.
31. Pramatarova L, Pecheva E, Krastev V, Riesz F. Ion implantation modified stainless steel as a substrate for hydroxyapatite deposition. Part I. Surface modification and characterization. J Mater Sci Mater Med. 2007; 18:435–40. [PubMed: 17334693]
32. Barrère F, van der Valk CM, Meijer G, Dalmeijer RAJ, de Groot K, Layrolle P. Osteointegration of biomimetic apatite coating applied onto dense and porous metal implants in femurs of goats. Journal of Biomedical Materials Research Part B: Applied Biomaterials. 2003; 67B:655–65.
33. León, B.; Jansen, JA. Thin calcium phosphate coatings for medical implants. New York: Springer; 2009.
34. Ducheyne P, Cuckler JM. Bioactive ceramic prosthetic coatings. Clin Orthop Relat Res. 1992:102–14. [PubMed: 1537141]
35. Tengvall P, Skoglund B, Askendal A, Aspenberg P. Surface immobilized bisphosphonate improves stainless-steel screw fixation in rats. Biomaterials. 2004; 25:2133–8. [PubMed: 14741628]
36. Skoglund B, Holmertz J, Aspenberg P. Systemic and local ibandronate enhance screw fixation. Journal of Orthopaedic Research. 2004; 22:1108–13. [PubMed: 15304286]
37. Wermelin K, Tengvall P, Aspenberg P. Surface-bound bisphosphonates enhance screw fixation in rats--increasing effect up to 8 weeks after insertion. Acta Orthop. 2007; 78:385–92. [PubMed: 17611854]

38. Andersson T, Agholme F, Aspenberg P, Tengvall P. Surface immobilized zoledronate improves screw fixation in rat bone: a new method for the coating of metal implants. J Mater Sci Mater Med. 2010; 21:3029–37. [PubMed: 20857321]
39. Wermelin K, Suska F, Tengvall P, Thomsen P, Aspenberg P. Stainless steel screws coated with bisphosphonates gave stronger fixation and more surrounding bone. Histomorphometry in rats. Bone. 2008; 42:365–71. [PubMed: 18055289]
40. Wermelin K, Aspenberg P, Linderbäck P, Tengvall P. Bisphosphonate coating on titanium screws increases mechanical fixation in rat tibia after two weeks. Journal of Biomedical Materials Research Part A. 2008; 86A:220–7. [PubMed: 17975821]
41. Abtahi J, Tengvall P, Aspenberg P. A bisphosphonate-coating improves the fixation of metal implants in human bone. A randomized trial of dental implants. Bone. 50:1148–51. [PubMed: 22348981]
42. Schilcher J, Koeppen V, Aspenberg P, Michaelsson K. Risk of atypical femoral fracture during and after bisphosphonate use. N Engl J Med. 2014; 371:974–6. [PubMed: 25184886]
43. Duarte PM, Cesar Neto JB, Goncalves PF, Sallum EA, Nociti jF. Estrogen deficiency affects bone healing around titanium implants: a histometric study in rats. Implant dentistry. 2003; 12:340–6. [PubMed: 14752971]
44. Lugero GG, de Falco Caparbo V, Guzzo ML, Konig B Jr, Jorgetti V. Histomorphometric evaluation of titanium implants in osteoporotic rabbits. Implant dentistry. 2000; 9:303–9. [PubMed: 11307552]
45. Ferris DM, Moodie GD, Dimond PM, Giorani CWD, Ehrlich MG, Valentini RF. RGD-coated titanium implants stimulate increased bone formation in vivo. Biomaterials. 1999; 20:2323–31. [PubMed: 10614938]
46. Schliephake H, Scharnweber D, Dard M, Rößler S, Sewing A, Meyer J, et al. Effect of RGD peptide coating of titanium implants on periimplant bone formation in the alveolar crest. Clinical Oral Implants Research. 2002; 13:312–9. [PubMed: 12010163]
47. Hennessy KM, Clem WC, Phipps MC, Sawyer AA, Shaikh FM, Bellis SL. The effect of RGD peptides on osseointegration of hydroxyapatite biomaterials. Biomaterials. 2008; 29:3075–83. [PubMed: 18440064]
48. Barber TA, Ho JE, De Ranieri A, Virdi AS, Sumner DR, Healy KE. Peri-implant bone formation and implant integration strength of peptide-modified p(AAM-co-EG/AAC) interpenetrating polymer network-coated titanium implants. Journal of Biomedical Materials Research Part A. 2007; 80A:306–20. [PubMed: 16960836]
49. Reyes CD, Garcia AJ. Engineering integrin-specific surfaces with a triple-helical collagen-mimetic peptide. J Biomed Mater Res A. 2003; 65:511–23. [PubMed: 12761842]
50. Reyes CD, Petrie TA, Burns KL, Schwartz Z, Garcia AJ. Biomolecular surface coating to enhance orthopaedic tissue healing and integration. Biomaterials. 2007; 28:3228–35. [PubMed: 17448533]
51. Petrie TA, Raynor JE, Reyes CD, Burns KL, Collard DM, Garcia AJ. The effect of integrin-specific bioactive coatings on tissue healing and implant osseointegration. Biomaterials. 2008; 29:2849–57. [PubMed: 18406458]
52. Marie PJ. Targeting integrins to promote bone formation and repair. Nat Rev Endocrinol. 2013; 9:288–95. [PubMed: 23358353]
53. Petrie TA, Reyes CD, Burns KL, Garcia AJ. Simple application of fibronectin-mimetic coating enhances osseointegration of titanium implants. J Cell Mol Med. 2009; 13:2602–12. [PubMed: 18752639]
54. Petrie TA, Capadona JR, Reyes CD, Garcia AJ. Integrin specificity and enhanced cellular activities associated with surfaces presenting a recombinant fibronectin fragment compared to RGD supports. Biomaterials. 2006; 27:5459–70. [PubMed: 16846640]
55. Schoen RC, Bentley KL, Klebe RJ. Monoclonal antibody against human fibronectin which inhibits cell attachment. Hybridoma. 1982; 1:99–108. [PubMed: 6208125]
56. Gregory CA, Grady Gunn W, Peister A, Prockop DJ. An Alizarin red-based assay of mineralization by adherent cells in culture: comparison with cetylpyridinium chloride extraction. Analytical Biochemistry. 2004; 329:77–84. [PubMed: 15136169]

57. McMillan J, Kinney RC, Ranly DM, Fatehi-Sedeh S, Schwartz Z, Boyan BD. Osteoinductivity of demineralized bone matrix in immunocompromised mice and rats is decreased by ovariectomy and restored by estrogen replacement. Bone. 2007; 40:111–21. [PubMed: 16973427]
58. Gao Y, Zou S, Liu X, Bao C, Hu J. The effect of surface immobilized bisphosphonates on the fixation of hydroxyapatite-coated titanium implants in ovariectomized rats. Biomaterials. 2009; 30:1790–6. [PubMed: 19135249]
59. Martino MM, Mochizuki M, Rothenfluh DA, Rempel SA, Hubbell JA, Barker TH. Controlling integrin specificity and stem cell differentiation in 2D and 3D environments through regulation of fibronectin domain stability. Biomaterials. 2009; 30:1089–97. [PubMed: 19027948]
60. Hamidouche Z, Fromigue O, Ringe J, Haupl T, Vaudin P, Pages JC, et al. Priming integrin alpha5 promotes human mesenchymal stromal cell osteoblast differentiation and osteogenesis. Proc Natl Acad Sci U S A. 2009; 106:18587–91. [PubMed: 19843692]
61. Marom R, Shur I, Solomon R, Benayahu D. Characterization of adhesion and differentiation markers of osteogenic marrow stromal cells. Journal of Cellular Physiology. 2005; 202:41–8. [PubMed: 15389528]
62. Yasothan U, Kar S. Osteoporosis: overview and pipeline. Nat Rev Drug Discov. 2008; 7:725–6. [PubMed: 19172687]
63. Jee WS, Yao W. Overview: animal models of osteopenia and osteoporosis. J Musculoskelet Neuronal Interact. 2001; 1:193–207. [PubMed: 15758493]
64. Keselowsky BG, Collard DM, Garcia AJ. Integrin binding specificity regulates biomaterial surface chemistry effects on cell differentiation. Proc Natl Acad Sci U S A. 2005; 102:5953–7. [PubMed: 15827122]
65. Javed F, Vohra F, Zafar S, Almas K. Significance of osteogenic surface coatings on implants to enhance osseointegration under osteoporotic-like conditions. Implant dentistry. 2014; 23:679–86. [PubMed: 25290281]
66. Halvorson TL, Kelley LA, Thomas KA, Whitecloud TS 3rd, Cook SD. Effects of bone mineral density on pedicle screw fixation. Spine (Phila Pa 1976). 1994; 19:2415–20. [PubMed: 7846594]
67. Weinstein JN, Spratt KF, Spengler D, Brick C, Reid S. Spinal pedicle fixation: reliability and validity of roentgenogram-based assessment and surgical factors on successful screw placement. Spine (Phila Pa 1976). 1988; 13:1012–8. [PubMed: 3206294]
68. Lopas L, Belkin N, Mutyaba P, Gray C, Hankenson K, Ahn J. Fractures in Geriatric Mice Show Decreased Callus Expansion and Bone Volume. Clin Orthop Relat Res. 2014; 472:3523–32. [PubMed: 25106797]

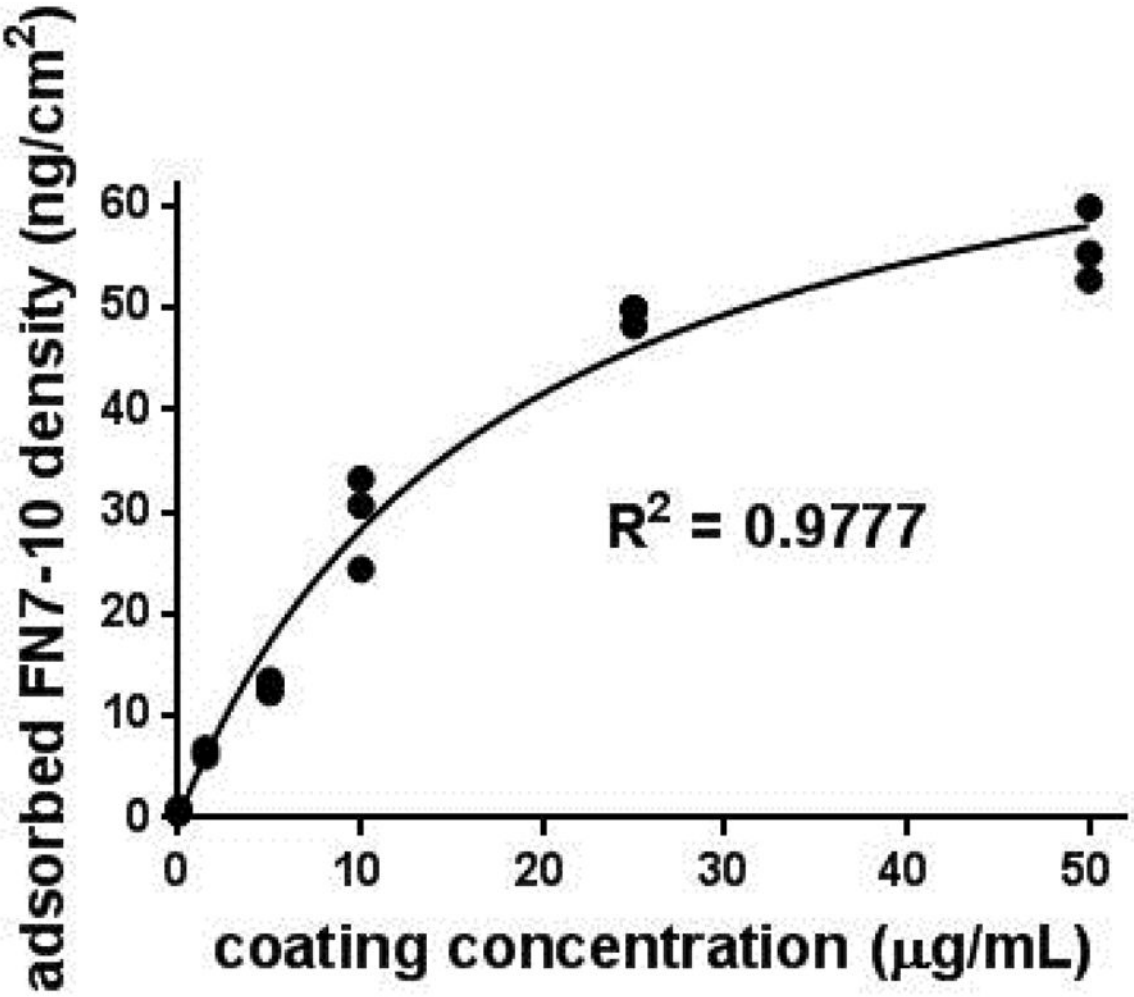

Figure 1.
FN7-10 adsorption onto SS coupons as a function of FN7-10 coating concentration. Hyperbolic curve-fit (ads density = 78.8 * conc/[17.9 + conc], R^2 = 0.98) shown.

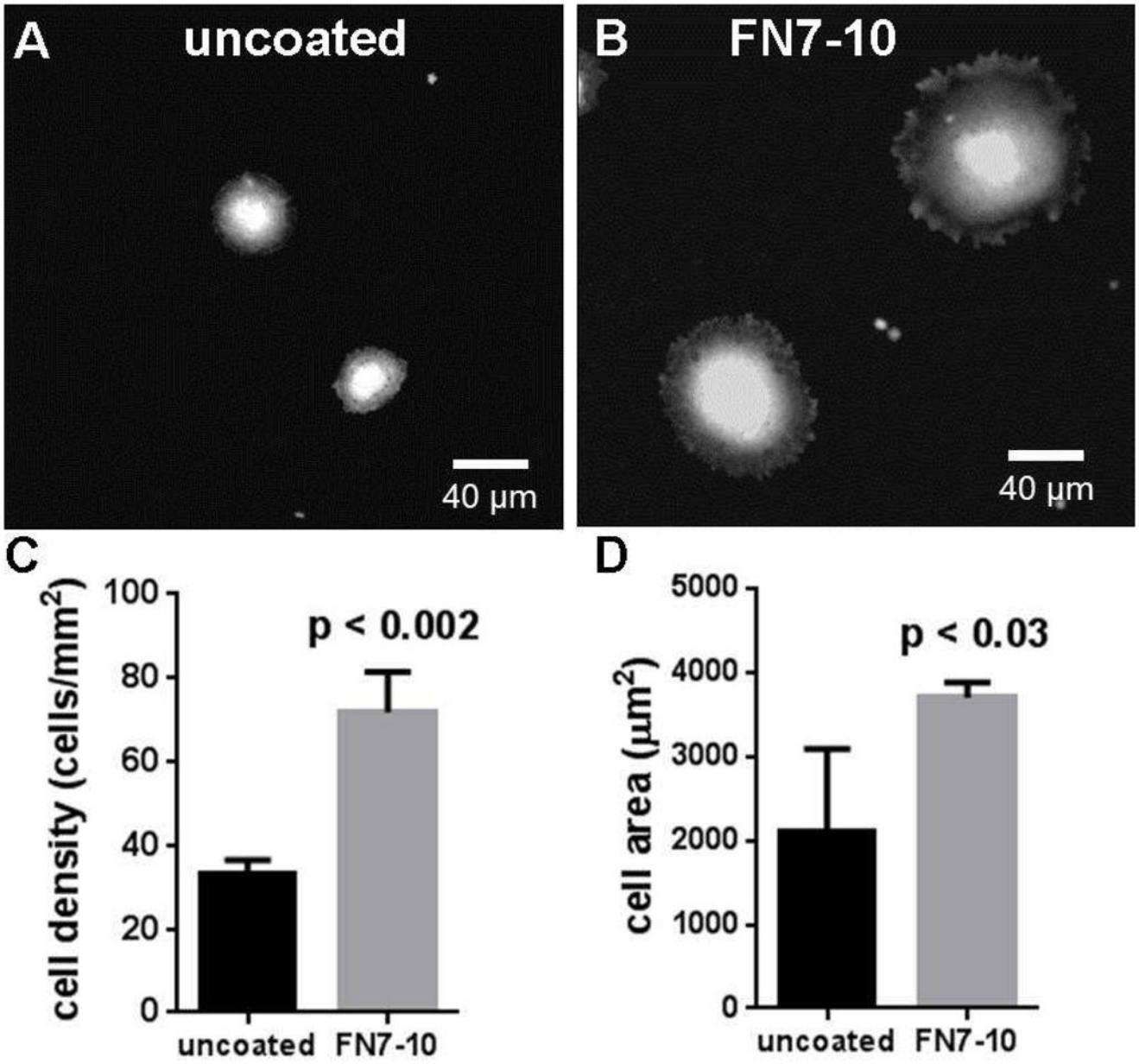

Figure 2.

FN7-10 coating enhances cell adhesion and spreading on SS. Fluorescence microscopy images of hMSCs stained with calcein and cultured on (A) uncoated SS and (B) FN7-10-coated SS. Quantification of (C) adherent cell density and (D) cell spreading area for hMSCs cultured on FN7-10-coated and uncoated surfaces.

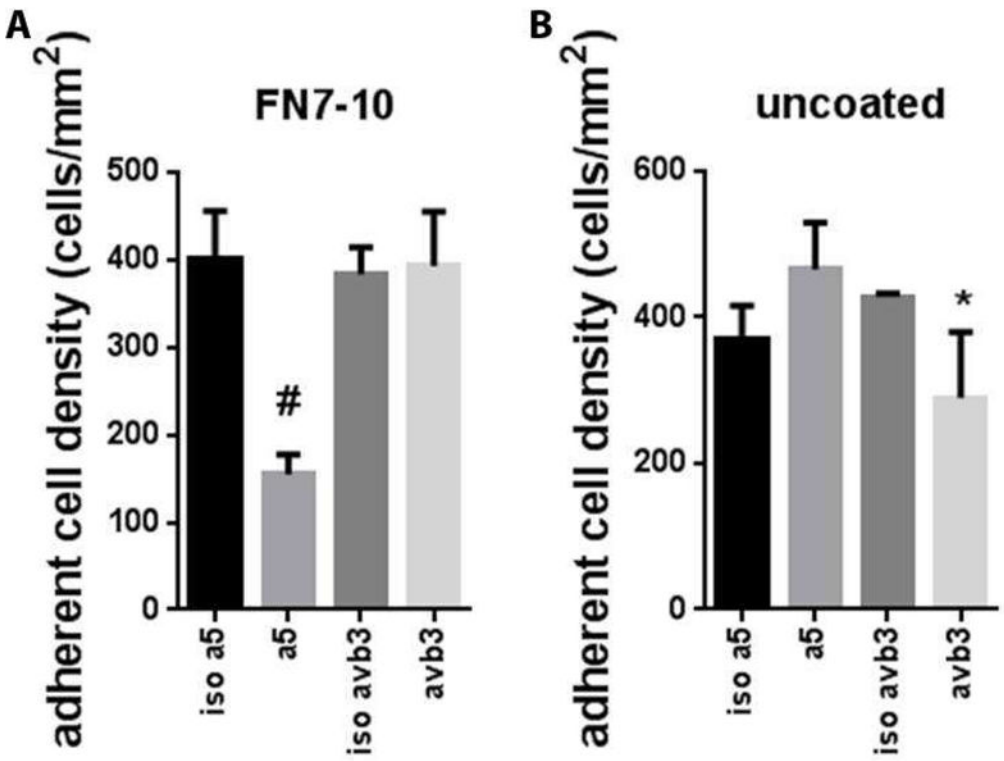

Figure 3.

Blocking studies with integrin-specific antibodies. Adherent cell density on (A) FN7-10-coated SS and (B) uncoated SS in the presence of blocking or isotype control antibodies. #$p < 0.002$ $\alpha 5$ vs. isotype control, * $p<0.05$ $\alpha v \beta 3$ vs. isotype control.

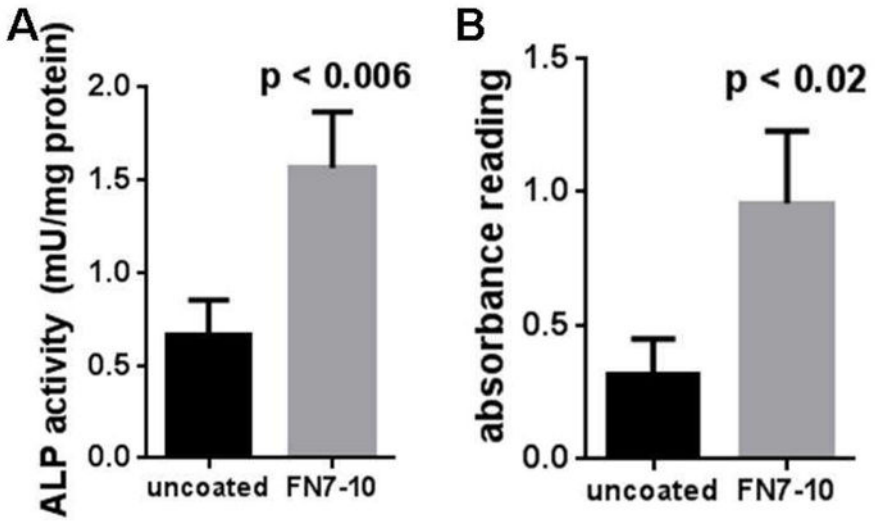

Figure 4.

FN7-10 coating enhances osteoblastic differentiation of hMSCs. (A) ALP activity at 9 days. (B) Alizarin red staining for mineralization at 21 days.

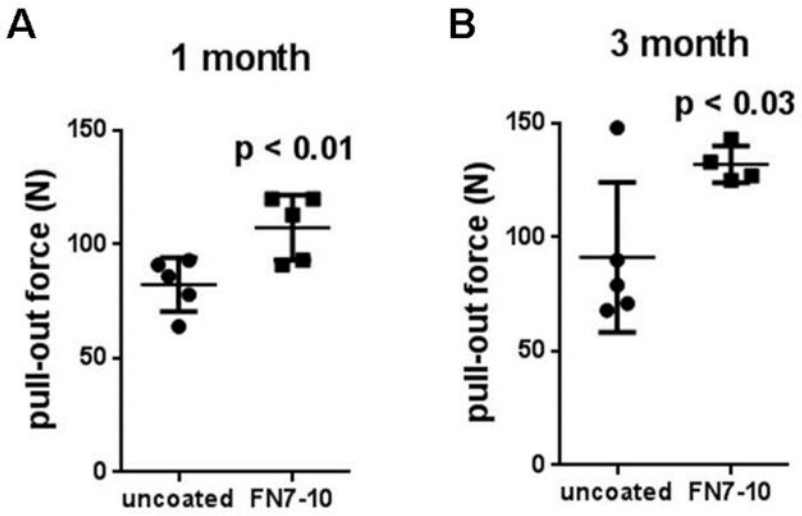

Figure 5.

Mechanical fixation of SS screws to bone as determined by pull-out force in healthy rats at (A) 1 month and (B) 3 months post-implantation. Experimental values (n=4–5 per group) and mean ± std deviation are shown.

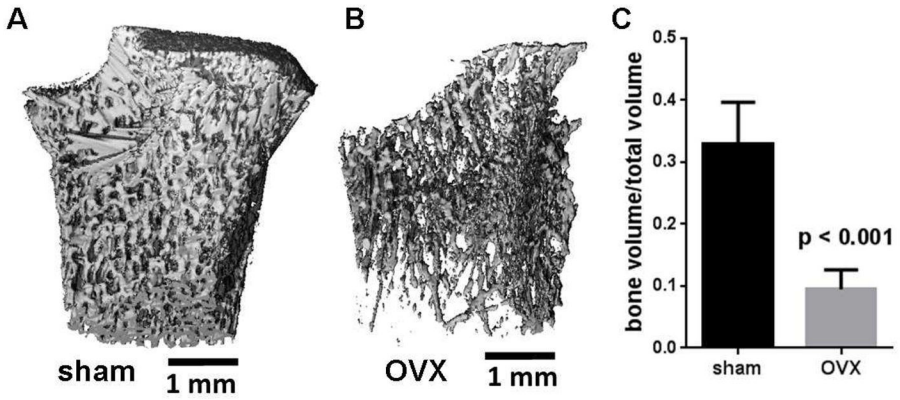

Figure 6.

Verification of osteoporotic state in ovariectomized rats. 3D μCT reconstructions of tibial metaphysis at 3 months after ovariectomy for (A) sham-operated and (B) ovariectomized (OVX) rats. C) Ratio of trabecular bone volume to total volume (BV/TV) 3 months after ovariectomy.

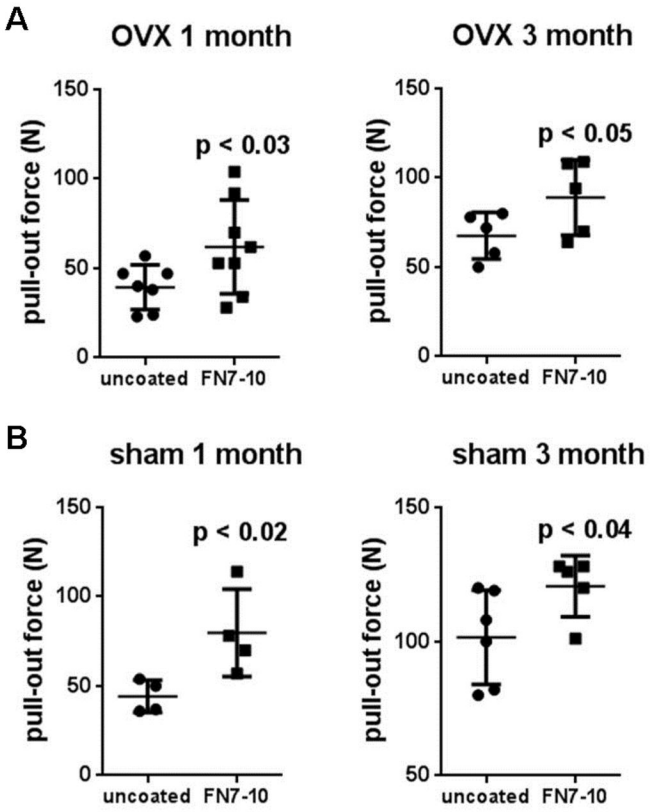

Figure 7.

Mechanical fixation of SS screws to bone as determined by pull-out force for (A) OVX and (B) sham-operated rats at 1 and 3 months post-implantation. Experimental values (n=5–8 per group for OVX, n=6–8 per group for sham-operated) and mean ± std deviation are shown.

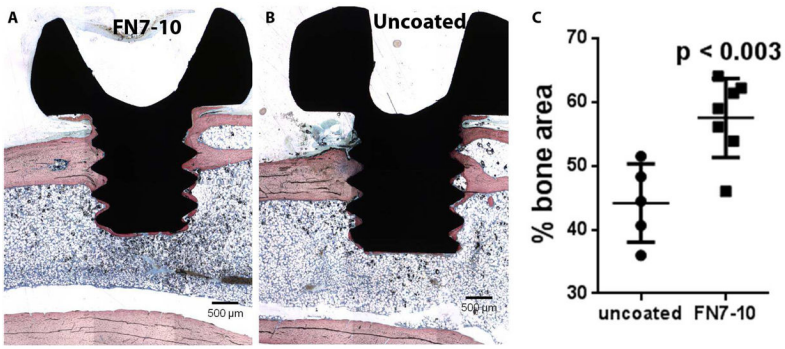

Figure 8.

Bone-implant contact and bone ingrowth into screw threads. Histological sections stained with Sanderson's Rapid Bone Stain and van Gieson counterstain from osteoporotic rats at 3 months postimplantation in osteoporotic rats for (A) FN7-10-coated and (B) uncoated SS screws. (C) Bone-implant contact and bone ingrowth into screw thread in osteoporotic rats after 3 post-implantation.